a

Design of a pre-stressed bridge deck with ultra-high performance concrete (UHPC)

Dimensionamento de um tabuleiro de uma ponte pré-esforçado em betão de ultra-elevado desempenho

Rui Valente
Gilberto Alves
Pedro Pacheco

Abstract

Two different bridge deck solutions using Ultra-High Performance Concrete (UHPC) are proposed. The existing design norms and guidelines are reviewed and compared. The constructive process and long-term effects were both considered in the numerical analysis. An auxiliary numerical tool was implemented to aid the design of the cross section. A bridge deck fully designed with UHPC (Case 1) and a mixed deck solution designed with both UHPC and conventional concrete (Case 2) are studied. Given the high strength grade of UHPC, the design strategy consisted in the reduction of structural elements thickness of the existing bridge deck. Both solutions allowed reducing considerably the deck weight, the amount of pre-stress and loads transmitted to the substructure. Case 2 showed to be more economic than Case 1 but less than the existing bridge. Further improvements in the economic assessment and possible design strategies are discussed.

Resumo

Neste trabalho são propostas duas soluções distintas para o tabuleiro de uma ponte em Betão de Ultra-Elevado Desempenho (UHPC). As normas e guias de dimensionamento são revistas e comparadas. O processo construtivo e os efeitos diferidos são tidos em conta na análise numérica. Uma ferramenta auxiliar foi implementada para apoiar o processo de dimensionamento da secção do tabuleiro. As duas soluções propostas consistem num tabuleiro unicamente dimensionado com UHPC (Caso 1) e numa solução mista onde betão convencional e UHPC são usados em conjunto (Caso 2). A estratégia de dimensionamento passou por reduzir a espessura dos elementos estruturais do tabuleiro da ponte existente. Ambas as soluções permitiram reduzir o peso do tabuleiro, a quantidade de pré esforço e a ação transmitida à subestrutura. O Caso 2 resultou numa solução mais económica que o Caso 1 mas menos que a solução existente. São discutidos aspetos adicionais a considerar na avaliação económica e possíveis estratégias de dimensionamento.

Keywords: Ultra-high performance concrete / Box girder / Structural design

Palavras-chave: Betão de Ultra-elevado desempenho / Viga-caixão / / Dimensionamento estrutural

Rui Valente

PhD Candidate
Faculdade de Engenharia da Universidade do Porto
Porto, Portugal
rui.v@fe.up.pt

Gilberto Alves

MSc in Civil Engineering
Faculdade de Engenharia da Universidade do Porto
Porto, Portugal
gilberto.alves@outlook.pt

Pedro Pacheco

Assistant Professor
Faculdade de Engenharia da Universidade do Porto
Porto, Portugal
pedro.pacheco@berd.eu

VALENTE, R. [*et al.*] – Design of a pre-stressed bridge deck with ultra-high performance concrete (UHPC). **Revista Portuguesa de Engenharia de Estruturas**. Ed. LNEC. Série III. n.º 14. ISSN 2183-8488. (novembro 2020) 19-28.

1 Introduction

Several experiments and studies were carried out in the past aiming to increase concrete strength. Most developments occurred during two decades between the 1970s and mid-1990s. Two major lines of research were followed aimed to achieve high mechanical performance with cementitious matrix materials. The first is concerned with high-strength densified with small particles (DSPs) concrete, including high superplasticizer, silica fume content and ultra-hard aggregate [1]. Another approach was oriented towards improving the strength of the paste, based on the concept of the so-called Micro-defected-free (MDF) paste [2]. High-strength DSPs concrete was developed further by scientific civision of *Bouygues* [3]. Steel straight fibers were added to the cementitious material matrix (2-2.5% per volume) and compressive strength reached 170 MPa. It was concluded that steel fibers enhanced ductile behaviour on rupture. Lafarge corporation developed a new mix formulation and labelled it as "Reactive Powder Concrete" (RCP) which continues to exist in the commercial form of "Ductal" [4].

After UHPC had become commercially available in the United States in 2000, it was applied in bridges in many ways, but the most common practice was to use it in bridge joints [5]. In 2002, France draw the first design recommendation on UHPC [6] and 2 years later Japan also released a comprehensive guideline [7]. Since 2005, large-scale research programs have been carried out in Germany [5] and in South Korea [8]. Malaysia UHPC bridge production is already taken seriously and 24 bridges made of UHPC were already been built in 2014 [9].

The history of structural engineering has shown that structural form is closely interrelated with the material of which it is made of. The emergence of new materials leads to new structural geometries so that the material properties can be fully exploited. Arches were early built with stone, then steel brought trusses, suspension and tied bridges. UHPC provides structural designers with distinct and improved mechanical properties. Thus, new structural concepts taking advantage of it are expected.

With the increasing mobility and accessibility needs comes a growing demand over infrastructures such as bridges. Consequently, the search for economical solutions is indispensable. UHPC is characterized by its compressive strength higher than 150MPa and tensile strength enhanced by steel fibers around 10MPa. Thus, it is required less material to resist the same loading. Consequently, lighter structures are expected to be designed when compared with those built with conventional concrete (CC). However, a major hindrance related with material high cost arises. Therefore, to evaluate whether UHPC application is economical or not, studies should be carried out.

The objective of this design is to use ultra-high performance concrete (UHPC) and assess if the common practice of reducing structural elements size/thickness for higher concrete grades either results or not in economic advantage. This work presents a possible bridge deck design approach based on relatively recent material with enhanced mechanical properties whose structural potential

should be assessed. The existing applicable standards are identified, compared, and used in the design process. When needed, existing research studies on the material behavior is used as complement.

2 UHPC

2.1 Composition

UHPC mixtures are typically designed with ordinary Portland cement. Fine quartz sand aggregate is frequently used and the most common maximum particle size of sand used is limited to over 5 or 6 mm [10, 11]. Quartz powder may equally be used with particle size distribution ranging from 0.1 to 100 μm and usually acts like a filler [12]. Silica fume with a typical diameter of 0.2 μm helps to occupy the space between the cement particles, to improve rheological behaviour and the formation of secondary hydrates. UHPC is distinguished by low water to bind ratio around 0.25 and silica fume content of 20% of the cement weight [13]. In order to reduce water content and to increase flowability, it is fundamental to add superplasticizers. However, setting time and early strength development is delayed by its presence [3]. Several types of steel fibers can be integrated in UHPC mixture. In the current work, steel fibers are assumed. Their geometry and content may vary from each supplier. Nevertheless, the purpose of using fibers is to increase ductility, strength and to reduce the cracking tendency [10].

2.3 Fresh state

Any CC mixer is capable of mixing UHPC but it demands more energy than CC does, meaning that mixing time should be longer. This fact combined with fine grain size and low water-binder ratio may lead to undesirable overheat during mixing [14]. Placing operations occupy a fundamental role on UHPC fibers orientation. Fiber reinforcement tends to show alignment preference on UHPC flow direction during casting and fibers close to walls tend to be oriented parallel to the formwork surface. Therefore, UHPC ultimate tensile strength and ductility are highly influenced by placement method [13] and this phenomenon must be considered during the development of casting sequence. The reduced water-binder ratio in a UHPC mix requires particular attention to prevent water to escape prior to hydration [14]. Additionally, the surface of constructive joints should be systematically cured so that both surface drying and micro-cracking may be prevented. Heat (90ºC) and steam (RH = 95%) treatment may be applied to UHPC to accelerate hydration process and to enhance mechanical properties including durability. These treatments are only feasible within a precast plant [15]. Hydration reaction starts 26h after water addition, approximately. This period is known by "dormant period" which is longer than that in CC because of significant amount of superplasticizer [16]. Mechanical properties start developing approximately 32h after water addition. After 7 days, the UHPC compressive strength achieves 140MPa (81% of final strength).

2.4 Hardened State

The typical compressive strength of UHPC ranges between 150 and 250MPa. UHPC shows linear elastic behaviour until 70 or 80 % of its ultimate compressive strength. The scatter of compressive strengths tests results is usually low due to homogeneity of the material [13]. The strain at peak stress is approximately 4.4 %. Thanks to the fibers, a pronounced descending branch towards rupture is developed (Figure 1). Its configuration is influenced by several factors: fiber content, orientation, geometry, stiffness and relation between fiber length and maximum aggregate dimension [17].

Graybeal and Baby [18] characterized uniaxial tensile response of UHPC specimen with strain hardening behaviour after a set of direct tension tests (Fig.1). The response can be divided into four phases. First, linear elastic domain (Phase I) is observed followed by the formation of multiples tightly spaced cracks which are bridged by steel fibers (Phase II). Cracks occur sequentially when the stress overpass the matrix cracking strength. When crack saturation occurs, individual cracks start to extend (Phase III). At certain moment, some crack reaches its extension limit and the bridging fibers begin to be pulled out from the matrix (Phase IV). This behaviour is known as strain-hardening. If the post-cracking strength is lower than the crack stress, the Phase IV comes right after the first cracking leading to a strain-softening material.

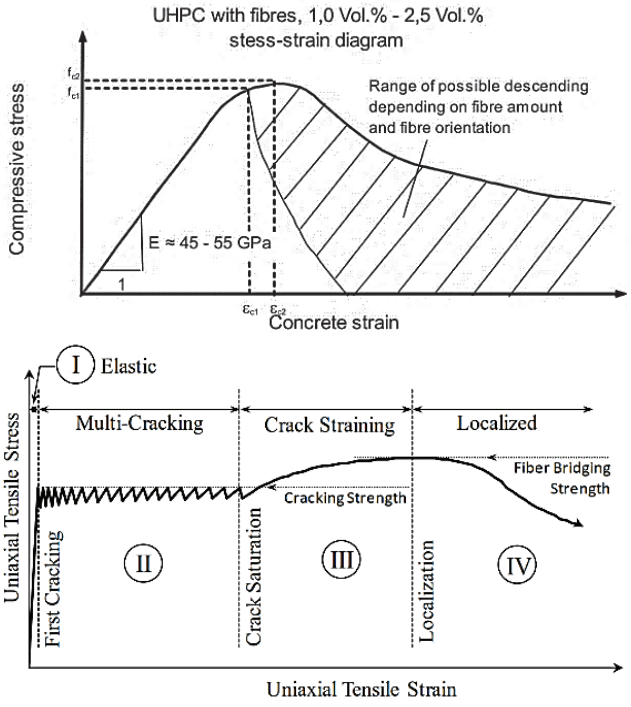

Figure 1 Typical stress-strain-diagrams of UHPC in compression (top) [17] and in tension (down) [18]

3 Design principles and assumptions

3.1 Standards

A reliable design must be supported by proper guidelines or codes. For that reason, a search for documents intended to support designers is performed as well as their review. Australian and Japanese documents are applicable in very limited cases. The former is suited for pre-stressed beams made of RPC [19], whereas the latter solely gives material properties to strict cure conditions and material mix [20]. The Swiss norm approaches several issues, but it is predominantly focused on pre-cast elements or reinforcement of existing structures [21]. Finally, France counts with expertise evidences in UHPC matters including regulation. In 2002, France came up with a complete recommendation for that time and which allowed engineers to design several bridges. Latter in 2013, it was updated mainly because of conformity reasons with Eurocode 2 (EC2) [15]. In 2016, France provided engineers with a national annex where every issue addressed in EC2 is also mentioned and reviewed for UHPC applications [22]. All in all, NF P 18-710 proves to be the most reliable and embracing UHPC design code. This document follows the previous French recommendations which had produced practical evidences of their application. That is why NF P 18-710 remain the primary reference during this case study.

3.2 Mechanical properties

The case study is carried out considering a field cast procedure, which means, no thermal treatment nor steam treatment. According to the NF P 18-710, this assumption has direct influence on shrinkage and creep values. According to the French norm [22], for preliminary or design studies, and in the absence of tests or an identity card of the material, it is possible to use the provided indicative values of UHPC properties at 28 days of age. Some of these values are tabulated in form of ranges and, for those, the minimum values are assumed. Higher strengths are usually attained under controlled curing conditions and eventually with heat treatment as in precast plants. However, the constructive method adopted presumes an *in-situ* cast. Additionally, the intermediate value for the fiber length was assumed (16 mm). The assumed properties are presented in the Table 1. This material will be described as UHPC150 henceforth, because of its characteristic compressive strength.

Table 1 Mechanical properties assumed for UHPC during the current study – UHPC150

Property	Symbol	Value
Elasticity Modulus	E_{cm}	45 GPa
Characteristic compressive strength	f_{ck}	150 MPa
Mean compressive strength	f_{cm}	160 MPa
Characteristic limit of elasticity under tension	$f_{ctk,el}$	7.0 MPa
Mean limit of elasticity under tension	$f_{ctm,el}$	8.0 MPa
Characteristic maximal post-cracking stress	f_{ctfk}	6.0 MPa
Mean maximal post-cracking stress	f_{ctfm}	7.0 MPa
Fibers' length	L_f	16 mm
Global fiber orientation factor	K_{global}	1.25
Local fiber orientation factor	K_{local}	1.75
Thermal expansion coefficient	α_t	11 μm/m/ºC
Crack opening corresponding to local peak	w_{pic}	0.3
Mean post-cracking stress corresponding to a crack width of 0.01H	$f_{ctf1\%}$	4.8 MPa
Crack width corresponding to the local peak in the curve	w_{pic}	0.3 mm
Crack width of 0.01H where H is the height of the tested prism	$w_{1\%}$	2 mm

3.3 Constitutive law for design

The compressive constitutive law is simply modelled with a bilinear diagram as depicted in the Figure 2. The derived parameters are presented in the Table 2. The plastic behavior is possible because of the post-cracking strength in the transverse direction which allows uniaxial compressive deformation under constant stress.

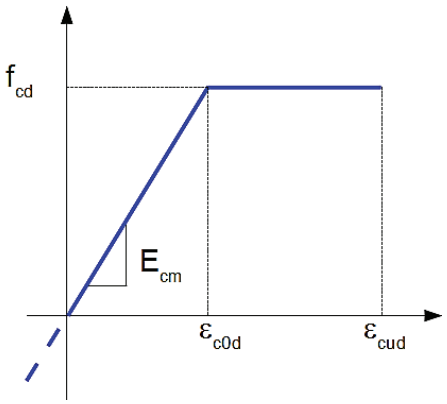

Figure 2 NF P 18-710 Design stress-strain relationship in compression [6]

In the framework of NF P 18-710, all structural elements to be designed in this work are classified as thick elements with strain-softening behavior. The corresponding tensile constitutive law is represented in the Figure 3. A safety factor (γ_{cf} = 1.3) is introduced regarding manufacturing defects and it is applied to tensile strength of UHPC. The post cracking constitutive law depends not exclusively on the material but also cross-section geometry, namely the cross-section depth (h). It is used to estimate the characteristic length (L_c) which relates the crack width to an equivalent deformation. It is employed as a reduction factor related to scale effect on the post-cracking strains. As an example, the values presented in the Table 2 are based on a cross-section depth of 25 cm. In order to take into account fibers variability in space and orientation, an additional reduction factor (K) is implemented. In a real design situation, and before implementing the validation process, the designer is allowed to use the recommended value of 1.25 for K factor. Next, suitability tests should be carried out to validate those values.

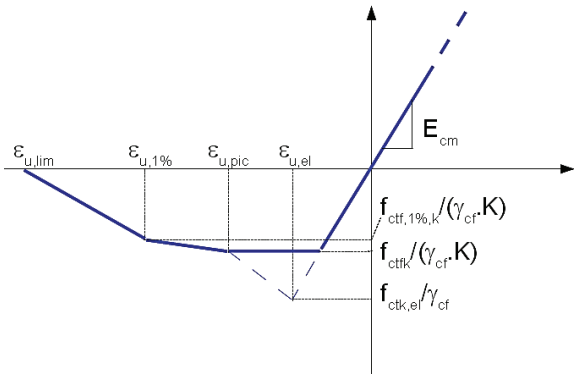

Figure 3 NF P 18-710 Design stress-strain relationship in tension [6]

Table 2 Mechanical properties assumed for UHPC during the current study – UHPC150

Compressive law		Tensile law	
α_{cc}	0.85	$L_c = \frac{2}{3}h$	16.7 cm
Υ_c	1.5	$f_{ctfk,u} = f_{ctfk}/(\gamma_{cf} K)$	3.7 MPa
$f_{cd} = \alpha_{cc} f_{ck}/\gamma_c$	85 MPa	$f_{ctf1\%,u} = 0{,}8\, f_{ctfk,u}$	3.0 MPa
$\varepsilon_{c0d} = f_{cd}/E_{cm}$	0.189%	$\varepsilon_{u,pic} = \frac{w_{peak}}{L_c} + \frac{f_{ctk,el}}{\gamma_{cf}\ E_{cm}}$	0.19%
$\varepsilon_{cud}\left[1+14\frac{f_{ctm}}{K_{global}\ f_{cm}}\right]\varepsilon_{c0d}$	0.295%	$\varepsilon_{u,1\%} = \frac{w_{1\%}}{L_c} + \frac{f_{ctk,el}}{\gamma_{cf}\ E_{cm}}$	1.21%
		$\varepsilon_{u,\lim} = \frac{w_f}{4L_c}$	2.40%

3.4 Time dependent properties

The way material strength and stiffness evolve during time has major importance during staged construction analysis. The results achieved by Habel et al. [16] in determining the models of mechanical properties development are used in this study. That paper is based in a proprietary UHPC (CEMTECmultiscale®) and proposes a model for the development of mechanical properties as function of degree of reaction (r) which, in turn, is function of time (t) – equation (1). Thus, any mechanical property "p" studied by Habel et al. can be modelled by the generic equation (2).

$$r = \frac{0.038(t-26)}{1+0.038(t-26)} \quad (1)$$

$$p(r) = \frac{(r-r_0)^a}{1-r_0} \times p(r=1) \quad (2)$$

Where r_0 is the degree of reaction at the beginning of the strength development, and takes the value of 0.16. The parameter a values 0.8, 1.1, 2.5 if the mechanical property being determined is either the elasticity modulus, compressive strength, limit of elasticity under tension, respectively [16]. The French norm provides indicative models for creep and shrinkage, and suggests intervals for the input parameters. Intermediate values were assumed. For more details on the models, refer to [22]. Finally, all time dependent data is inputted on structural analysis software which performs step-by-step calculation as described by the general method mentioned in EN1992-2 for the assessment of structural effects of time dependent behavior [23].

3.5 Bending calculation

A numerical tool following the strategy of *Yoo and Yoon* [24] was implemented in a worksheet aiming to aid the sectional analysis given the complexity of the post-cracking constitutive law. It is based on the assumption of linear strain distribution (Figure 4). The constitutive laws of UHPC and steel reinforcement are used to find the stresses distribution. The stresses are numerically integrated along the cross-section depth. The minimum required steel reinforcement was found in each case by stablishing equilibrium between internal and applied forces and iteratively changing the position of neutral axis (*c*) and the curvature (Φ). To better illustrate the method, the Annex I presents the results of particular design example of a 0.25 m thick slab under pure bending moment of 260 kN.m/m.

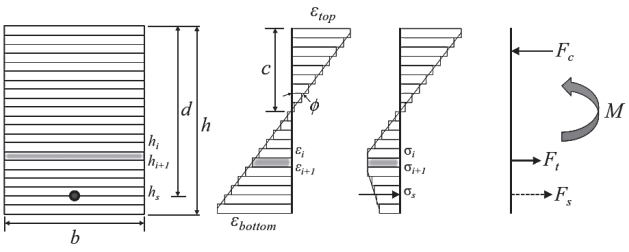

Figure 4 Schematic explanation of stress and strain distributions in cross-section [24]

3.6 Shear

NF P 18-710 allows the superposition of shear strength given by matrix, shear reinforcement and fibers. The shear strength component due to fibers bridging cracks is given by the equation (3).

$$V_{Rd,f} = A_{fv}\,\sigma_{Rd,f}\,\cot\theta \qquad (3)$$

Where A_{fv} is the cross-section area delimited by the lever arm of the internal forces (*z*), and $\sigma_{Rd,f}$ is the mean value of the post-cracking stress resistance along the shear crack. Both UHPC matrix and shear reinforcement contribution to shear strength are determined similarly to that is described on EC2. However, when determining the compressed strut strength, no positive direct influence provided by pre-stressing is considered, contrary to what is described in EC2.

4 Case study: Río Cabriel Bridge

4.1 Existing bridge

The present bridge of the current case study was constructed in 2010. It is placed in Spain (Cofrentes, Valencia). It integrates the national road N-330 and passes over the Cabriel river. It has 8 spans which totals 520 m length. The common span has 70 m of length and 11 m of width. The tallest pier is approximately 45 m high. The superstructure is a concrete box girder with 2.5 m depth at mid-span (Figure 5) whereas it reaches 3.47 m over the piers.

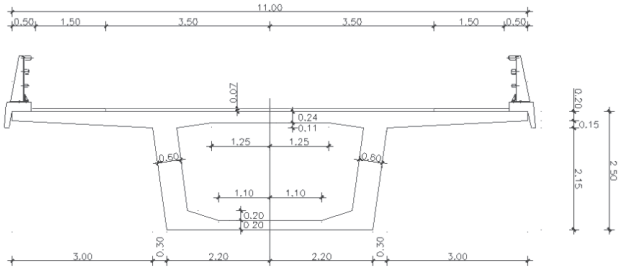

Figure 5 Río Cabriel Bridge - Cross-section at mid span

4.2 Load cases

Each stage of constructive process was considered in the numerical calculation. The equipment considered was the Movable Scaffolding System M70-S developed by *BERD – Bridge Engineering Research & Design*. The evolving superstructure scheme, self-weight, construction equipment loads and pre-stressing action were applied sequentially and according to the construction time schedule of the existing bridge. The reduced loads imposed by constructive equipments on the structure due to the deck mass reduction during the design process is properly considered. The remaining permanent loads, thermal loads and traffic loads were defined during service stage. All load cases are defined according to European Norms. Finally, by combining all load cases, it was possible to output internal forces, stresses and deflections for ultimate and serviceability limit state design and verifications.

4.3 Design

For simplicity, the cross-section geometry was kept constant along the deck length. The depth of the cross-section was fixed to 2.5m. This value leads to a slenderness of L/h = 28, which is between those adopted for the box girders of the *Batu 6 Bridge* (25) and *PS34 Bridge* (30) [25, 26]. External pre-stressing solution was adopted in order to remove constructive limitations to the reduction of web thickness. Tendons' layout (Figure 6) has two configurations. The polygonal configuration is intended to balance vertical loads. The straight tendons segments over the piers were required to reduce high negative bending moments and deflections that arise during the construction stage.

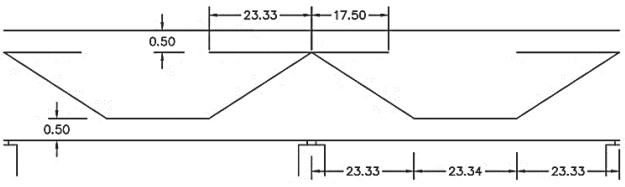

Figure 6 External tendons lay-out [m]

In the Case 1, the superstructure is solely materialized with UHPC along its length. The thickness of the webs and flanges were iteratively reduced as long as the limit states are verified during the constructive

and service phases. The amount of reinforcement was also limited in order to meet constructive requirements concerning the minimum bar spacing. The resulting cross-section is presented in the Fig. 6. The concept of the Case 2 consists of placing the UHPC where the deck is under more demanding bending and shear forces, i.e. near the piers. The remaining deck is casted with CC. The reasoning is analogous to the design of lightened slabs where a solid slab is placed near the supports to resist high internal forces. However, in this case, it would be the strength of the material changing instead of the cross-section (Figure 7).

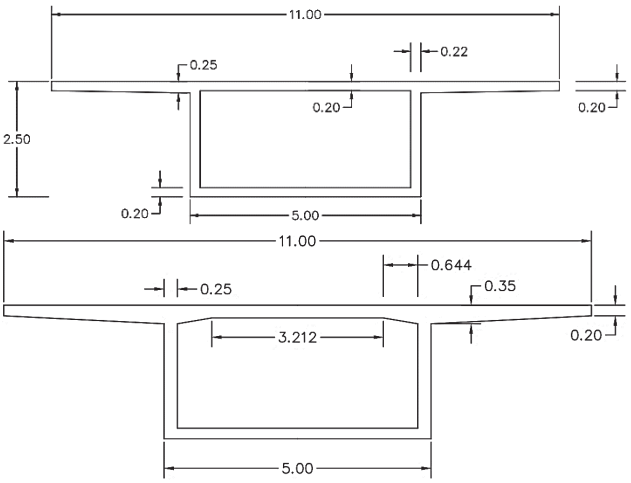

Figure 7 Cross-section solution of Case 1 (top) and Cross-section solution of Case 2 (down)

Since the structural elements became slenderer the need for considering second-order effects was verified. Two buckling analysis were performed. The first was performed during the construction phase whereas the second was performed during the service phase. For simplicity, a partial model of the deck was used for numerical analysis and the geometric imperfections were disregarded. In both situations, the main buckling mode occurs in the bottom flange close to the pier (Figure 8). The minimum buckling factor of 13.4 which lead to conclude that the second-order effects can be disregarded.

4.4 Comparative analysis

When compared to the existing bridge deck (Case 0), the axial force transmitted to the piers under quasi-permanent combination of loads was reduced on average by 24% for Case 1 and 18% for Case 2. The Table 3 shows the percentage variation of the base reactions for each seismic type in both longitudinal and transverse directions of the bridge deck. The seism type 1 is the governing one. Significant horizontal action reductions were only observed in the transverse direction. The reductions observed also mean that shear and bending moments transferred to the piers and foundations decrease.

Table 3 Percentage change of global base reactions when compared with Case 0 [%]

Case	Seismic type 1		Seismic type 2	
	ΔF long.	ΔF tansv.	ΔF long.	ΔF transv.
1	+ 0.9	– 14.6	– 26.9	– 14.4
2	– 0.9	– 8.0	– 19.8	– 7.7

Those reductions are justified by the decrease of the superstructure mass of 36% for Case 1 and 26% for Case 2 (Table 4).

Table 4 Amount of concrete and/or UHPC

Case	Area	C 40/50		UHPC 150	
		Volume	Mass	Volume	Mass
	[m²]	[m³]	[t]	[m³]	[t]
0	6.67	3441	8777	–	–
1	4.27 (– 36%)	–	–	2220	5663
2	4.95 (– 26%)	1151	2934	1423	3627

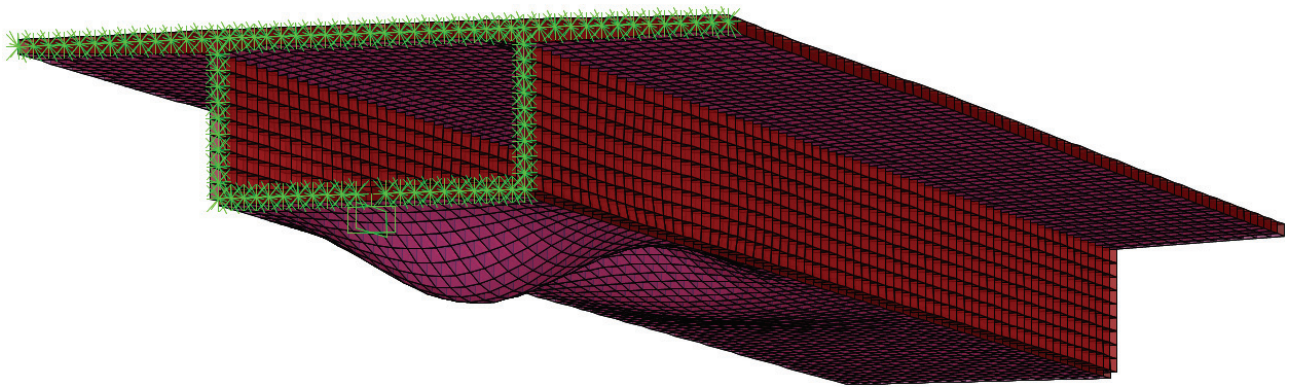

Figure 8 Case 2 - Buckling mode during constructive process

The amount of pre-stress tendons is also reduced by 36% and 32% (Table 5), respectively. The amount steel reinforcement was not accounted for due to the lack of information about the original project.

Table 5 Amount of pre-stressing steel

Case	Total length	Volume	Mass
	[m]	[m³]	[t]
0	193440	27.08	212.6
1	123904 (– 36%)	17.35	136.2
2	131184 (– 32%)	18.47	145.0

There is significant scatter on UHPC unit cost [27] when compared with CC. For that reason, the study is carried on by considering two limit unit costs: 500 (scenario 1) and 2000 €/m³ (scenario 2). Additionally, the conventional concrete C40/50 was assumed to costs 95€/m³ and the pre-stressing streel is assumed to cost 2800€/t. The Figure 9 illustrates stacked column charts where partial and total costs are placed side by side for each case in each scenario. The reduction of mass was not enough to outweigh the high cost of UHPC. Therefore, both proposed solutions for the deck did not present economic advantage.

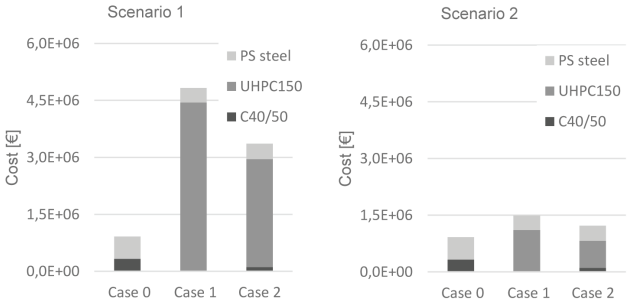

Figure 9 Partial and total costs of the scenario 1 (left) and the scenario 2 (right)

5 Conclusion

As expected, the enhanced mechanical properties provided by UHPC materials lead to slenderer structural elements. The optimization process adopted consisted on the progressive reduction of the thickness of webs and flanges as much as the material strength and limit states allowed. The present standards covered almost every design aspect of this study case. However, the mechanical parameters should be carefully handled, mainly those referring to post-cracking constitutive law. The design should be supported by experimental tests accounting for structural geometry and casting method because of their influence on fibers distribution.

Adopting the structural elements thickness as the main optimization variable did not result in economic feasibility of the deck solutions in the Case 1 and 2. The trend observed on the deck cost from case 1 to case 2 suggests that further rationing of the UHPC should be carried out so it can be allocated where it is most effective. The contribution of the post-cracking tensile strength provided by UHPC is higher in shear and flexural design of thin elements, e.g., the design of the top slab in the transverse direction (Annex I). Due to scale-effect, the steel fibers do not contribute as much in the design of thicker/tall elements like the cross section of a bridge deck. Moreover, UHPC high compressive strength can only be fully exploit in the highly compressed bottom flanges close to the piers.

There are other aspects to be considered in future studies and that might lead to different conclusions. The steel reinforcement was not considered in the economical assessment. NF P18-710 states that all minimum reinforcement quantities are no more applicable to UHPC structures due to its improved ductility. There might be cases where it is possible to design unreinforced elements leading to less costs associated to rebar working and placement as well. Moreover, the constructive equipment might be adjusted to bear less fresh concrete and consequently the action of its self-weight on the superstructure is expected to decrease as well. A multivariable optimization where aspects such as cross-section configuration, structural scheme, span length, pre-stressing solution and layout should be accounted for in future similar studies. Lastly, a global economic study including the substructure elements is suggested since they are less loaded.

Acknowledgements

I would like to thank to BERD - Bridge Engineering Research & Design for all the support during the development of this work, including the details about the case study bridge and the Movable Scaffolding System M70-S.

References

[1] Bache, H. – *Densified cement ultra-fine particle-based materials*. 1981, Aalborg, Portland.

[2] Birchall, J., *et al.* – *Flexural strength and porosity of cements*. Nature, 1981. 289(5796): p. 388-390.

[3] Richard, P.; Cheyrezy, M. – *Composition of reactive powder concretes*. Cement and concrete research, 1995. 25(7): p. 1501-1511.

[4] Fehling, E., *et al.* – *Ultra-High Performance Concrete UHPC: Fundamentals, Design, Examples*. 2014: John Wiley & Sons.

[5] Russell, H.G., et al. – *Ultra-high performance concrete : a state-of-the-art report for the bridge community*. 2013, McLean, VA: U.S. Department of Transportation, Federal Highway Administration, Research, Development, and Technology, Turner-Fairbank Highway Research Center.

[6] Thibaux, T. – UHPFRC Development: *The Experience of BSI® Applications. Designing and Building with UHPFRC*, 2010: p. 63-76.

[7] Uchida, Y., *et al.* – *Outlines of" Recommendations for Design and Construction of Ultra High Strength Fiber Reinforced Concrete Structures*" by JSCE. in International RILEM Workshop on High Performance Fiber Reinforced Cementitious Composites in Structural Applications. 2006. RILEM Publications SARL.

[8] Kim, B., *et al. – R&D activities and application of ultra high performance concrete to cable-stayed bridges*. in Proceedings of Hipermat 2012 3rd International Symposium on UHPC and Nanotechnology for High Performance Construction Materials, Kassel University Press, Kassel. 2012.

[9] Voo, Y.L., *et al. – Ultrahigh-performance concrete segmental bridge technology: Toward sustainable bridge construction*. Journal of Bridge Engineering, 2014.

[10] Orgass, M.; Klug, Y. – *Fibre reinforced ultra-high strength concretes*. in Proceedings of the International Symposium on Ultra High Performance Concrete. Kassel, Germany. 2004.

[11] Camacho, E., *et al. – Definition of three levels of performance for UHPFRC-VHPFRC with available materials*. in Proceedings of Hipermat 2012 3rd International Symposium on UHPC and Nanotechnology for High Performance Construction Materials, Kassel University Press, Kassel. 2012.

[12] Heinz, D., *et al. – Effect of heat treatment method on the properties of UHPC*. in Proceedings of Hipermat 2012 3rd International Symposium on UHPC and Nanotechnology for High Performance Construction Materials, Kassel University Press, Kassel. 2012.

[13] Resplendino, J. – *Introduction: What is a UHPFRC? Designing and Building with UHPFRC*, 2011: p. 3-14.

[14] Graybeal, B. – *Ultra-high performance concrete*. 2011.

[15] AFGC, S. – *Bétons fibrés à ultra-hautes performances – Recommandations, in Recommandations*. 2013.

[16] Habel, K., *et al. – Development of the mechanical properties of an ultra-high performance fiber reinforced concrete (UHPFRC)*. Cement and Concrete Research, 2006. 36(7): p. 1362-1370.

[17] Fehling, E., *et al. – Design relevant properties of hardened ultra high performance concrete*. in Proceedings of the International Symposium on Ultra High Performance Concrete. Kassel, Germany. 2004.

[18] Graybeal, B.A.; Baby, F. – *Development of Direct Tension Test Method for Ultra-High-Performance Fiber-Reinforced Concrete*. ACI Materials Journal, 2013. 110(2).

[19] Gowripalan, N.; Gilbert, R. – *Design Guidelines for Ductal Prestressed Concrete Beams*. Design Guide. Civil & Environmental Engineering School, University of NSW, Sydney, Australia, 2000.

[20] Uchida, Y., *et al. – Outlines of "Recommendations for Design and Construction of Ultra High Strength Fiber Reinforced Concrete Structures*" by JSCE. in International RILEM Workshop on High Performance Fiber Reinforced Cementitious Composites in Structural Applications. 2006. RILEM Publications SARL.

[21] Société S. des Ingénieurs e des Architectes – *Béton fibré ultra-performant (BFUP) - Matériaux, dimensionnement et exécution*, in prSIA 2052 :2014-04. 2014.

[22] AFNOR – Calcul des structures en béton – *Règles spécifiques pour les bétons fibrés à ultra-hautes performances in Complément national à l'Eurocode 2*. 2016: France.

[23] Hendy, C.R.; Smith, D.A. – *Designers' Guide to EN 1992-2: Eurocode 2: Design of Concrete Structures*. Concrete bridges. 2007: Thomas Telford.

[24] Yoo, D.-Y.; Yoon, Y.-S – *Structural performance of ultra-high-performance concrete beams with different steel fibers*. Engineering Structures, 2015. 102: p. 409-423

[25] Voo, Y.L.; Foster, S.J. – *Design and Construction of the 100 metre Span UHPC Batu 6 Segmental Box Girder Bridge, in Proceedings of Hipermat 2016 – 4th International Symposium on Ultra-High Performance Concrete and High Performance Construction Materials Kassel*. 2016, Kassel University Press: Kassel, Germany

[26] Delauzun, O., *et al.*, – Construction of the PS34 UHPFRC bridge. Designing and building with UHPFRC, 2011: p. 137-148.

[27] Wille, K.; Graybeal, B. – *Development of Non-Proprietary Ultra-High Performance Concrete for Use in the Highway Bridge Sector*. 2013

Annex

UHPC 150				
x_i	$b_{(xi)}$	$\varepsilon_{(xi)}$	$\sigma_{(xi)}$	$F_{(xi)}$
[M]	[m]	(-)	[kPa]	[kN]
0.00125	1.00	– 0.00171	-77087	– 193
0.00375	1.00	– 0.0016	– 72058	– 180
0.00625	1.00	– 0.00149	– 67030	– 168
0.00875	1.00	– 0.00138	– 62001	– 155
0.01125	1.00	– 0.00127	– 56973	– 142
0.01375	1.00	– 0.00115	– 51944	– 130
0.01625	1.00	– 0.00104	– 46916	– 117
0.01875	1.00	– 0.00093	-41887	– 105
0.02125	1.00	-0.00082	-36859	– 92
0.02375	1.00	-0.00071	-31831	– 80
0.02625	1.00	-0.0006	– 26802	– 67
…	…	…	…	…
0.22875	1.00	0.00846	3219	8
0.23125	1.00	0.00857	3211	8
0.23375	1.00	0.00868	3203	8
0.23625	1.00	0.00879	3195	8
0.23875	1.00	0.0089	3187	8
0.24125	1.00	0.00901	3179	8
0.24375	1.00	0.00913	3171	8
0.24625	1.00	0.00924	3162	8
0.24875	1.00	0.00935	3154	8

Variables	
φ [m^{-1}]	0.04469
x [m]	0.0396

Reinforcement	
A_s [m^2]	1.96 E-03
d_s [m]	0.21
σ_s [kPa]	434783
F_s [kN]	852

Internal Forces	
$M = \Sigma(F_{(xi)}\, x_i) + F_s\, d_s$	260 kN.m
$N = \Sigma F_{(xi)}$	0 kN

The numerical tool can be also used to draw the Bending moment-Curvature diagram: